Inorg. Chem. **2003**, *42*, 1688–1700

Electronic Tuning of the Lability of Pt(II) Complexes through π-Acceptor Effects. Correlations between Thermodynamic, Kinetic, and Theoretical Parameters

Andreas Hofmann,[†] Deogratius Jaganyi,[†,‡] Orde Q. Munro,[‡] GUnter Liehr,[†] and Rudi van Eldik*[,†]

Institute for Inorganic Chemistry, University of Erlangen-Nürnberg, Egerlandstr. 1, 91058 Erlangen, Germany, and School of Chemical and Physical Sciences, University of Natal, Private Bag X01, Pietermaritzburg 3209, South Africa

Received October 7, 2002

π-Acceptor effects are often used to account for the unusual high lability of $[Pt(terpy)L]^{(2-n)+}$ (terpy = 2,2′:6′,2″-terpyridine) complexes. To gain further insight into this phenomenon, the π-acceptor effect was varied systematically by studying the lability of $[Pt(diethylenetriamine)OH_2]^{2+}$ (**aaa**), $[Pt(2,6\text{-bis-aminomethylpyridine})OH_2]^{2+}$ (**apa**), [Pt(*N*-(pyridyl-2-methyl)-1,2-diamino-ethane)OH_2]$^{2+}$ (**aap**), $[Pt(bis(2\text{-pyridylmethyl})amine)OH_2]^{2+}$ (**pap**), [Pt(2,2'-bipyridine)-$(NH_3)(OH_2)$]$^{2+}$ (**app**), and $[Pt(terpy)OH_2]^{2+}$ (**ppp**). The crystal structure of the **apa** precursor [Pt(2,6-bis-aminomethylpyridine)Cl]Cl·H_2O was determined. The substitution of water by a series of nucleophiles, viz. thiourea, *N*,*N*-dimethylthiourea, *N*,*N*,*N*′,*N*′-tetramethylthiourea, I^-, and SCN^-, was studied under pseudo-first-order conditions as a function of concentration, pH, temperature, and pressure, using stopped-flow techniques. The data enable an overall comparison of the substitution behavior of these complexes, emphasizing the role played by the kinetic *cis* and *trans* π-acceptor effects. The results indicate that the *cis* π-acceptor effect is larger than the *trans* π-acceptor effect, and that the π-acceptor effects are multiplicative. DFT calculations at the B3LYP/LACVP** level of theory show that, by the addition of π-acceptor ligands to the metal, the positive charge on the metal center increases, and the energy separation of the frontier molecular orbitals ($E_{LUMO} - E_{HOMO}$) of the ground state Pt(II) complexes decreases. The calculations collectively support the experimentally observed additional increase in reactivity when two π-accepting rings are adjacent to each other (**app** and **ppp**), which is ascribed to "electronic communication" between the pyridine rings. The results furthermore indicate that the pK_a value of the platinum bound water molecule is controlled by the π-accepting nature of the chelate system and reflects the electron density around the metal center. This in turn controls the rate of the associative substitution reaction and was analyzed using the Hammett equation.

Introduction

Following Rosenberg's discovery of the antitumor properties of cis-platin in 1969,[1] studies on the substitution behavior of Pt(II) complexes have attracted much attention. Since cis-platin was only active against some specific cancers, new drugs had to be developed for possible application in the treatment of other types of cancer. Two approaches were adopted: a wide variety of different Pt(II) complexes were synthesized and tested for their possible biological activity; systematic investigations were launched in efforts to resolve the factors that control the reactivity (lability) of Pt(II) complexes.[2] Once such factors are well understood, it should in principle be possible to design Pt(II) complexes with specific kinetic and thermodynamic properties to reach a desired activity in specific biological environments.

Such studies have shown that steric hindrance above and below the square-planar plane of the Pt(II) complex can significantly slow the rate of the substitution reaction,[3−5]

* To whom correspondence should be addressed. E-mail: vaneldik@chemie.uni-erlangen.de.
† University of Erlangen-Nürnberg.
‡ University of Natal.

(1) Rosenberg, B.; Van Champ, L.; Trosko, J. E.; Mansour, V. H. *Nature* **1969**, *22*, 385.
(2) *Cisplatin: chemistry and biochemistry of a leading anticancer drug*; Lippert, B., Ed.; Wiley-VCH: Weinheim, 1999.
(3) Romeo, R.; Minniti, D.; Trozzi, M. *Inorg. Chim. Acta* **1975**, *14*, L15.
(4) Romeo, R.; Minniti, D.; Trozzi, M. *Inorg. Chem.* **1976**, *15*, 1134.

10.1021/ic020605r CCC: $25.00
Published on Web 01/30/2003

whereas steric crowding in the plane of the complex can result in an increase in reactivity.[6,7] In addition, many studies have focused on the electronic tuning of the reactivity of Pt(II) complexes by changing the nature of the ligand *trans* to the reactive site. The observed trend depending on the selected system is an increase (even as high as 10^{11}-fold) in the lability of the investigated complexes for stronger *trans* labilizing ligands.[8−14] It has been shown that the *trans*-effect consists of σ- and π-contributions,[14] the first can be seen in a ground state labilization (*trans*-influence),[13] the latter in a transition state stabilization.[9] Although many studies on the *trans*-effect have been performed, considering both σ- and π-contributions, the influence of π-acceptors only has not been studied in as much detail, except for the case of Zeise's anion, $[PtCl_3(C_2H_4)]^-$, where the ligand exchange kinetics *trans* to the very strong π-acceptor ethylene have been studied in detail.[9] π-Acceptor effects in general have been shown to play an important role in Pt(II) chemistry.[17−22] It is known that the complex $[Pt(terpy)(L)]^{(2-n)+}$ (terpy = 2,2′:6′,2″-terpyridine) shows a very high lability relative to the corresponding $[Pt(dien)(L)]^{(2-n)+}$ (dien = diethylenetriamine, the terpy complex being 10^4-10^5 times more labile), which is assigned to π-back-bonding from the metal to the empty π^*-orbitals of the pyridine subunits of the terpy ligand.[23−25] Another possible reason offered for this high reactivity is the steric strain on the $[Pt(terpy)(L)]^{(2-n)+}$ complexes.[26]

Despite all the evidence for the influence of π-accepting pyridine ligands on the electronic properties of the Pt(II) center, no investigation (apart from our recent preliminary report,[27] and a recent study dealing with some similar complexes[28]) has been performed in which a systematic variation of the π-acceptor effect by replacing amines with π-accepting pyridines in tridentate N-donor systems was undertaken. Since this effect seems to play a major role in going from $[Pt(dien)(L)]^{(2-n)+}$ to $[Pt(terpy)(L)]^{(2-n)+}$ complexes, and both complexes are of biological interest in terms of their cytotoxicity,[29,30] it seemed appropriate to study the behavior of these types of complexes in more detail. We therefore investigated the effect of a systematic displacement of amine donors by π-accepting pyridines in tridentate N-donor chelates (of the dien and terpy type) on the thermodynamic and kinetic behavior of Pt(II) complexes. The reactions were all studied in aqueous solution, in order to be able to employ the gained insight in the design of antitumor drugs. We studied the substitution behavior of the corresponding aqua complexes, since these are considered to be the reactive species in the key step of the binding of cis-platin to DNA.[2] Furthermore, with a neutral leaving group, it is possible to prevent charge separation/neutralization effects that could complicate the mechanistic interpretation of the kinetic activation parameters.

From a systematic variation of the influence of mainly one factor (viz. the π-accepting ability of the chelate) on the substitution lability, it was possible to observe some important trends that are often hidden in other studies by stronger σ-donor or steric effects. We have clearly observed a decrease in electron density on the Pt(II) center, an increase in the ability of the complex to stabilize further incoming electron density on the Pt(II) center, and a decrease in the energy separation of the frontier molecular orbitals in these Pt(II) complexes, with increasing number of π-acceptors in the coordination sphere, which in turn affected the kinetic and thermodynamic parameters that control the ligand substitution process. In addition, our observations enable a systematic comparison of *cis* and *trans* π-acceptor effects of pyridine rings in ligand substitution reactions, and the introduction of an acceleration concept based on "electronic communication" between the π-accepting pyridine rings.

Experimental Section

Chemicals and Ligands. The ligands diethylenetriamine, bis-(2-pyridylmethyl)amine, 2,2′-bipyridine, and 2,2′:6′,2″-terpyridine were obtained from Aldrich. All other chemicals were of the highest purity commercially available. All chemicals were used without further purification. Ultrapure water was used for the kinetic as well as spectroscopic measurements.

2,6-Bis-aminomethylpyridine was prepared following a method used to synthesize 6-(aminomethyl)-2,2′-bipyridine[31] by using 2,6-bis(bromomethyl)pyridine[32] as starting material. A solution of 2,6-bis(bromomethyl)pyridine (4.76 g, 18 mmol) in 30 mL of chloroform was added dropwise to a solution of hexamethylenetetramine (5.5 g, 39.2 mmol) in chloroform (100 mL) over a period of 3 h

(5) Krüger, H.; van Eldik, R. *J. Chem. Soc., Chem. Commun.* **1990**, 330.
(6) Romeo, R.; Scolaro, L. M.; Nastasi, N.; Arena, G. *Inorg. Chem.* **1996**, *35*, 5087.
(7) Clark, R. J. H.; Fanizzi, F. P.; Natile, G.; Pacifico, C.; van Rooyen, C. G.; Tocher, D. A.; *Inorg. Chim. Acta* **1995**, *235*, 205.
(8) Gosling, R.; Tobe, M. L. *Inorg. Chem.* **1983**, *22*, 1235.
(9) Otto, S.; Elding, L. I. *J. Chem. Soc., Dalton Trans.* **2002**, 2354.
(10) Cusumano, M.; Marricchi, P.; Romeo, R.; Ricevuto, V.; Belluco, U. *Inorg. Chim. Acta* **1979**, *34*, 169.
(11) Schmülling, M.; Ryabov, A. D.; van Eldik, R. *J. Chem. Soc., Dalton Trans.* **1994**, 1257.
(12) Schmülling, M.; Grove, D. M.; van Koten, G.; van Eldik, R.; Veldman, N.; Spek, A. L. *Organometallics* **1996**, *15*, 1384.
(13) Wendt, O. F.; Elding, L. I. *Inorg. Chem.* **1997**, *36*, 6028.
(14) Wendt, O. F.; Elding, L. I. *J. Chem. Soc., Dalton Trans.* **1997**, 4725.
(15) Plutino, M. R.; Scolaro, L. M.; Romeo, R.; Grassi, A. *Inorg. Chem.* **2000**, *39*, 2712.
(16) Romeo, R.; Grassi, A.; Scolaro, L. M. *Inorg. Chem.* **1992**, *31*, 4383.
(17) Cornioley-Deuschel, C.; von Zelewsky, A. *Inorg. Chem.* **1987**, *26*, 3354.
(18) Blanton, C. B.; Rillema, D. P. *Inorg. Chim. Acta* **1990**, *168*, 145.
(19) Blanton, C. B.; Murtaza, Z.; Shaver, R. J.; Rillema, D. P. *Inorg. Chem.* **1992**, *31*, 3230.
(20) Chen, Y.; Merkert, J. W.; Murtaza, Z.; Woods, C.; Rillema, D. P. *Inorg. Chim. Acta* **1995**, *240*, 41.
(21) Zheng, G. Y.; Rillema, D. P. *Inorg. Chem.* **1998**, *37*, 1392.
(22) Maresca, L.; Natile, G. *Comments Inorg. Chem.* **1993**, *14* (6), 349−66.
(23) Mureinik, R. J.; Bidani, M. *Inorg. Chim. Acta* **1978**, *29*, 37.
(24) Pitteri, B.; Marangoni, G.; Cattalini, L.; Bobbo, T. *J. Chem. Soc., Dalton Trans.* **1995**, 3853.
(25) Romeo, R.; Plutino, M. R.; Scolaro, L. M.; Stoccoro, S.; Minghetti, G. *Inorg. Chem.* **2000**, *39*, 4749.
(26) Basolo, F.; Gray, H. B.; Pearson, R. G. *J. Am. Chem. Soc.* **1960**, *82*, 4200.
(27) Jaganyi, D.; Hofmann, A.; van Eldik, R. *Angew. Chem., Int. Ed.* **2001**, *40*, 1680.
(28) Pitteri, B.; Marangoni, G.; Cattalini, L.; Visentin, F.; Bertolasi, V.; Gilli, P. *Polyhedron* **2001**, 20, *869*.
(29) Palmer, B. D.; Wickham, G.; Craik, D. J.; McFadyen, W. D.; Wakelin, L. P. G.; Baguley, B. C.; Denny, W. A. *Anti-Cancer Drug Des.* **1992**, *7* (5), 385.
(30) Lowe, G.; Droz, A. S.; Vilaivan, T.; Weaver, G. W.; Tweedale, L.; Pratt, J. M.; Rock, P.; Yardley, V.; Croft, S. L. *J. Med. Chem.* **1999**, *42* (6), 999.
(31) Ziessel, R.; Lehn, J.-M *Helv. Chim. Acta* **1990**, *73*, 1149.
(32) Baker, W.; Buggle, K. M.; McOmie; J. F. W.; Watkins; D. A. M. *J. Chem. Soc.* **1958**, 3594.

while the mixture was being stirred under reflux. This produced a white precipitate that formed instantly. The reaction mixture was left to stir under reflux for $2^1/_2$ days for more product to form. This was then cooled to room temperature and the white crude product collected by filtration, washed three times with 10 mL portions of chloroform, and dried under vacuum giving 9.6 g (17,6 mmol) of crude white 2,6-bis-hexaminiummethylpyridine bromide (yield 98%).

The intermediate product was converted to 2,6-bis-aminomethylpyridine without further purification. A 4.8 g (8.8 mmol) portion of 2,6-bis-hexaminiummethylpyridine bromide was added to a mixture of 200 mL of ethanol and 30 mL of concentrated hydrochloric acid. The suspension was stirred under reflux for another $2^1/_2$ days, followed by solvent removal through rotary evaporation, and the sample, a mixture of ammonium chloride and the ligand, was dried under vacuum. The mixture was dissolved in 60 mL of 40% NaOH and the solution extracted 5 times with 20 mL portions of chloroform. The organic phases were combined and the solvent removed by rotary evaporation leaving an oily substance which was dissolved in 2-propanol (50 mL). Dropwise addition of a solution of HCl (2.8 mL concentrated HCl in ca. 25 mL 2-propanol) produced the precipitate of the desired compound. This was collected by filtration, washed several times with small portions of 2-propanol, and dried under vacuum. The ligand was recrystallized from a hydrochloric acid/methanol mixture (1:25), giving the wanted white 2,6-bis-aminomethylpyridine·2HCl (422 mg, 2 mmol, yield 23%). Anal. Calcd for $C_7H_{13}Cl_2N_3$: H, 6.2; C, 40.0; N, 20.0. Found: H, 6.59; C, 39.83; N, 19.10. ^{1}H NMR (D_2O, 300 K): δ 7.91 (t, $^3J_{HH}$ = 7.8 Hz, 1 H, para), δ 7.44 (d, $^3J_{HH}$ = 7.9 Hz, 2 H, meta), δ 4.38 (s, 4 H, CH_2).

***N*-(Pyridyl-2-methyl)-1,2-diamino-ethane** was synthesized following a literature method,[33] but with a modified purification procedure. A 2 mL portion of the oily product obtained after distillation was dissolved in 50 mL of 2-propanol. A layer of 2.6 mL of HCl in 40 mL of 2-propanol was carefully introduced to the bottom of the solution and the mixture stored in the refrigerator for 3 days. The precipitate that formed was collected by filtration and washed three times with 5 mL portions of 2-propanol. The yellow powder was recrystallized from a hydrochloric acid/methanol mixture (1:25) to give the required white *N*-(pyridyl-2-methyl)-1,2-diamino-ethane·3HCl product. Anal. Calcd for $C_8H_{16}Cl_3N_3$: H, 6.19; C, 36.87; N, 16.12. Found: H, 6.63; C, 36.49; N, 15.78. ^{1}H NMR (D_2O, 300 K): δ 8.64 (d, $^3J_{HH}$ = 4.9 Hz, 1 H, ortho), δ 8.00 (t, $^3J_{HH}$ = 7.9 Hz, 1 H, para), δ 7.59 (d,$^3J_{HH}$ = 7.7 Hz, 1 H, meta), δ 7.55 (t, $^3J_{HH}$ = 6.3 Hz, 1 H, meta), δ 4.47 (s, 2 H, benzyl-CH_2), δ 3.39 (t, $^3J_{HH}$ = 5.1 Hz, 2 H, CH_2), δ 3.36 (t,$^3J_{HH}$ = 5.1 Hz, 2 H, CH_2).

Synthesis of Complexes. Literature procedures were used for the synthesis of Pt(COD)Cl_2,[34] [Pt(diethylenetriamine)OH_2]$(CF_3SO_3)_2$ (**aaa**),[35] [Pt(bipy)(NH_3)Cl]ClO_4,[36] and [Pt(terpyridine)OH_2]$(BF_4)_2$ **(ppp)**.[37]

[Pt(*N*-(pyridyl-2-methyl)-1,2-diamino-ethane)Cl]Cl. A solution of *N*-(pyridyl-2-methyl)-1,2-diamino-ethane·3HCl (350 mg, 1.343 mmol) in 0.1 M NaOH (15 mL) was added to a water (30 mL) suspension of Pt(COD)Cl_2 (502.5 mg, 1.343 mmol). The mixture was stirred at 55−60 °C and the pH adjusted to 3.5 every 30 min by addition of NaOH (0.1 M). After 4 h, a clear solution was obtained. The stirring was continued overnight at room temperature, after which the solution was filtered and taken to dryness by rotary evaporation. The resulting solid was recrystallized twice from water and washed very carefully with small amounts of water, ethanol, and diethyl ether. Yield: 245 mg (0.51 mmol, 38%). Anal. Calcd for $C_8H_{13}Cl_2N_3O_4Pt$: H, 2.72; C, 19.97; N, 8.73. Found: H, 2.86; C, 20.02; N, 8.55. ^{1}H NMR: δ 8.69 (d, $^3J_{HH}$ = 5.7 Hz, $^3J_{PtH}$ 26.4 Hz, 1 H, ortho), δ 8.12 (t,$^3J_{HH}$ = 7.9 Hz, 1 H, para), δ 7.57 (d,$^3J_{HH}$ = 7.6 Hz, 1 H, meta), δ 7.49 (t,$^3J_{HH}$ = 6.5 Hz, 1 H, meta), δ 4.49 (dd,$^3J_{HH}$ = 34.2 Hz, $^4J_{HH}$ = 15.6 Hz, 2 H, benzyl-CH_2), δ 3.31−2.93 (m, 4 H, CH_2−CH_2).

[Pt(2,6-bis-aminomethylpyridine)Cl]Cl·H_2O. A suspension of Pt(COD)Cl_2 (600 mg, 1.60 mmol) in 20 mL of water and a solution of 2,6-bis-aminomethylpyridine·2HCl (336.9 mg, 1.60 mmol) in 15 mL 0.1 of M NaOH, was stirred at 60 °C. The pH was adjusted to 7.0 every 30 min by addition of NaOH (0.1 M). After 5 h, when the solution maintained a constant pH, a drop of concentrated HCl was added to give a pH of 2.8. The solution was filtered and concentrated by removal of most of the solvent through rotary evaporation. The required product was then allowed to crystallize out of the remaining solution (ca. 10 mL) by keeping the content in the refrigerator overnight. The solution was decanted, and the yellow crystals that formed (of X-ray quality) were washed carefully with acetone. Yield: 318 mg (47%). Anal. Calcd for $C_7H_{13}Cl_2N_3OPt$: H, 3.09; C, 19.95; N, 9.98. Found: H, 3.21; C, 19.86; N, 9.86. ^{1}H NMR (D_2O, 300 K): δ 8.07 (t,$^3J_{HH}$ = 8.0 Hz, 1 H, para), δ 7.41 (d,$^3J_{HH}$ = 7.9 Hz, 2 H, meta), δ 4.61 (s, $^3J_{PtH}$ = 27.0 Hz, 4 H, CH_2).

[Pt(2,6-bis-aminomethylpyridine)OH_2]$(SO_3CF_3)_2$ (apa). To a solution of $AgCF_3SO_3$ (143.7 mg, 0.559 mmol) in 15 mL of water in a dark reaction vessel was added a solid sample of [Pt(2,6-bis-aminomethylpyridine)Cl]Cl·H_2O (118.3 mg, 0.281 mmol). The mixture was stirred at 50 °C for 18 h. The white precipitate that formed (silver chloride) was filtered off using a Millipore filtration unit, and the solution was taken to dryness by rotary evaporation to give the expected white powder. Yield: 144 mg (0.222 mmol, 79%). Anal. Calcd for $C_9H_{13}F_6N_3O_7PtS_2$: H, 1.92; C, 16.67; N, 6.48. Found: H, 2.0; C, 16.52; N, 6.26. ^{1}H NMR (D_2O, 300 K): δ 8.06 (t,$^3J_{HH}$ = 8.0 Hz, 1 H, para), δ 7.39 (d,$^3J_{HH}$ = 8.0 Hz, 2 H, meta), δ 4.64 (s, $^3J_{PtH}$ 25.0 Hz, 4 H, CH_2).

[Pt(bis(2-pyridylmethyl)amine)Cl]ClO_4. To a suspension of Pt(COD)Cl_2 (52 mg, 0.14 mmol) in water (30 mL) was added 29 μL of bis(2-pyridylmethyl)amine (28 mg, 0.14 mmol). The pH was then adjusted to 3.5 by addition of concentrated HCl. The mixture was heated to 60 °C while continuously being stirred and was maintained at this temperature until the solution was clear. This was later filtered and 2 mL of saturated $NaClO_4$ solution added. The yellow compound formed, [Pt(bis(2-pyridylmethyl)amine)Cl]ClO_4, was filtered off and washed carefully with small amounts of water, ethanol, and ether after which it was dried under vacuum to give the analytically pure material. Yield: 21 mg (0.04 mmol 29%). Anal. Calcd for $C_{12}H_{13}Cl_2N_3O_4Pt$: H, 2.46; C, 27.22; N, 7.94. Found: H, 2.55; C, 27.50; N, 7.62. ^{1}H NMR (D_2O, 300 K): δ 8.80 (d,$^3J_{HH}$ = 5.9 Hz, 2 H, ortho, broad Pt satellite shoulders), δ 8.15 (t,$^3J_{HH}$ = 7.5 Hz, 2 H, para), δ 7.63 (d,$^3J_{HH}$ = 8.2 Hz, 2 H, meta), δ 7.51 (t,$^3J_{HH}$ = 7.0 Hz, 2 H, meta), δ 4.88 (s, 4 H, CH_2).

[Pt(bis(2-pyridylmethyl)amine)OH]ClO_4 (pap). [Pt(bis(2-pyridylmethyl)amine)Cl]ClO_4, (216 mg, 0.39 mmol) was dissolved in hot water (50 mL). To the clear solution was added 5 mL of 0.1 M NaOH. This resulted in a color change from yellow to green.

(33) Barger, J. D.; Zachariasen, R. D.; Romary, J. K. *J. Inorg. Nucl. Chem.* **1969**, *31*, 1019.
(34) McDermott, J. X.; White, J. F.; Whitesides, G. M. *J. Am. Chem. Soc.* **1976**, *98*, 6521.
(35) Fairlie, D. P.; Jackson, W. G.; Skelton, B. W.; Wen, H.; White, A. H.; Wickramasinghe, W. A.; Woon, T. C.; Taube, H. *Inorg. Chem.* **1997**, *36*, 1020.
(36) Morgan, G. T.; Burstall, F. H. *J. Chem. Soc.* **1934**, 965.
(37) Annibale, G.; Bergamini, P.; Bertolasi, V.; Cattabriga, M.; Lazzaro, A.; Marchi, A.; Vertuani, G. *J. Chem. Soc, Dalton Trans*. **1999**, 3877.

The solution was then heated to 80 °C and the temperature maintained for 20 min with continuous stirring. The desired product was precipitated out of the solution by adding 4 mL of saturated $NaClO_4$. The yellow powder that formed after the mixture had been stored in the refrigerator overnight was filtered off, washed carefully with small amounts of water, and dried under vacuum to give [Pt(bis(2-pyridylmethyl)amine)OH]ClO_4. Yield: 159 mg (80%). Anal. Calcd for $C_{12}H_{14}N_3ClO_5Pt$: H, 2.74; C, 28.2; N, 8.2. Found: H, 2.73; C, 28.2; N, 7.97. ^{1}H NMR (D_2O, 300 K): δ 8.46 (d, $^3J_{HH}$ = 5.7 Hz, 2 H, ortho, broad Pt satellite shoulders), δ 8.17 (t, $^3J_{HH}$ = 7.9 Hz, 2 H, para), δ 7.62 (d,$^3J_{HH}$ = 8.0 Hz, 2 H, meta), δ 7.56 (t,$^3J_{HH}$ = 6.8 Hz, 2 H, meta), δ 4.74 (s, 4 H, CH_2).

[Pt(bis(2-pyridylmethyl)amine)OH_2]$(ClO_4)_2$ (aap) and [Pt(bipy)$(NH_3)(OH_2)$]$(ClO_4)_2$ (app).[38] The two aqua complexes (**aap**) and (**app**) were prepared from their corresponding chloro complexes by removing the chloride ion using $AgClO_4$. A known amount of the corresponding chloro complex was dissolved in aqueous solution (0.1 M $NaClO_4$, pH = 2−3, $HClO_4$) to give a concentration of 1.0 mM. An almost stoichiometric amount (99%) of $AgClO_4$ was then added to the solution and the resulting mixture stirred for 16 h at 50 °C in the dark. The AgCl precipitate was filtered off using a Millipore filtration unit. The solution collected was diluted with ultrapure water (I = 0.1 ($NaClO_4$), pH = 2 ($HClO_4$)) to the desired concentration for the kinetic and spectroscopic investigations.

X-ray Structure Determination. Intensity data were collected on a Nonius CAD4 Mach3 diffractometer with graphite monochromated Mo Kα radiation in the $\omega/2\theta$ scan mode at room temperature. The structure of [Pt(2,6-bis-aminomethylpyridine)Cl]Cl·H_2O was solved by direct methods using SIR-928[39] and refined by full-matrix least-squares on F^2 using SHELXL-97.[40] Complete crystallographic details, bond lengths, bond angles, anisotropic temperature factors, and hydrogen atom coordinates are available as a CIF file as Supporting Information. Experimental lattice constants and SHELXL-97 refinement parameters for the structure are given in the following paragraph.

[Pt(2,6-bis-aminomethylpyridine)Cl]Cl·H_2O. $C_7H_{13}Cl_2N_3OPt$, fw = 421.181 g mol^{-1}, a = 7.073(5) Å, b = 8.747(5) Å, c = 9.812(5) Å, α = 73.28(2)°, β = 81.50(2)°, γ = 78.10(2)°, V = 566.3(6) Å^3, triclinic $P\bar{1}$, Z = 2, D_c = 2.435 g cm^{-3}, μ = 12.8 mm^{-1}, T = 293(2) K, R1 = 0.036 for data with $F_o > 2\sigma(F_o)$,[41] R1(wR2) = 0.045(0.109) for all data (R_{int} = 0.074 for 2247 unique reflections). The maximum and minimum electron densities on the final difference Fourier map were 2.06 and −1.466 e A^{-3}, respectively.

Instrumentation and Measurements. NMR spectroscopy (Bruker Avance DPX 300) and a Carlo Erba elemental analyzer 1106 were used for chemical analysis and complex characterization. UV−vis spectra for the determination of pK_a values and for the study of slow reactions were recorded on a Varian Cary 5G spectrophotometer equipped with a thermostated cell holder or on a Shimadzu UV-2101-PC spectrophotometer with a thermoelectrically temperature controlled cell holder. The pH of the solutions was measured using a Mettler Delta 350 digital pH meter, which had a combination glass electrode. This electrode was calibrated using standard buffer solutions of pH 4, 7, and 9 obtained from Sigma.

Kinetic measurements on fast reactions were studied on an Applied Photophysics SX 18MV stopped-flow instrument coupled to an online data acquisition system. The wavelengths used for each reaction are listed in Table S1 (see Supporting Information). Experiments at elevated pressure (1 to 130 MPa) were performed on a laboratory-made high-pressure stopped-flow instrument.[42] The temperatures of the instruments were controlled at an accuracy of ±0.1 °C, while the ionic strength of the solution was maintained at 0.1 M using $NaClO_4$. The ligand substitution reactions were studied under pseudo-first-order conditions. This was achieved by using at least a 10-fold excess of the nucleophile. The exception was the reaction between [Pt(dien)OH_2]$^{2+}$ and TMTU, where the complex was used in excess due to the strong absorbance of TMTU. All the reported rate constants represent an average value of at least six kinetic runs for each experimental condition.

DFT Calculations. Density functional theory (DFT) calculations (pseudospectral method,[43−45] B3LYP functional,[46] LACVP** basis set,[47] medium grid) were performed with Jaguar 4.0[48] running on a Compaq Alpha Station DS20e. The LACVP basis set employs effective core potentials for the elements K−Cu, Rb−Ag, Cs−La, and Hf−Au. Second and third row s- and p-block elements are described by Pople's 6-31G** basis set.[49,50] Due to the paucity of X-ray crystal structures of [Pt(L)(OH_2)]$^{2+}$ complexes, where L = terpy or a neutral tridentate N-donor ligand, in the Cambridge Structural Database (CSD), the X-ray structures of [Pt(terpy)(OMe)]$^+$ [51] and [Pt(apa)Cl]$^+$ were used to gauge the performance of the DFT calculations at the chosen level of theory. In both cases, the X-ray fractional coordinates were converted to Cartesian coordinates with ORTEP-3[52] and the crystal structures used as input for the calculations. Full geometry optimizations to a gradient convergence limit of 4.500 × 10^{-4} (no symmetry restrictions) were carried out before a final single point calculation. The converged DFT wave functions for each complex were analyzed with Weinhold's NBO 4.M program[53] which uses the first-order reduced density matrix of the wave function to obtain natural atomic orbitals (NAOs) and natural electron populations for the system. Input structures for **ppp**, **aaa**, **aap**, **apa**, **pap**, and **app** were obtained by modification/editing of the refined coordinates of [Pt(terpy)(OMe)]$^+$ and [Pt(apa)Cl]$^+$ with HyperChem 5.02[54] before transfer to Jaguar

(38) This complex was chosen instead of the corresponding chelate complex, because the synthesis of the 6-(amino-methyl)-2,2'-bipyridine ligand is rather complicated and very time-consuming

(39) Altomare, A.; Cascarano, G.; Giacovazzo, C.; Guagliardi, A.; Burla, M. C.; Polidori, G.; Camalli, M. SIR-92-Program Package for Solving Crystal Structures by Direct Methods. *J. Appl. Crystallogr.* **1994**, *27*, 435.

(40) Sheldrick, G. M. *SHELXL-97*; University of Göttingen: Göttingen, Germany, 1997. (a) Sheldrick, G. M. *Acta Crystallogr., Sect A* **1990**, *A46*, 467−473. (b) Sheldrick, G. M. *Acta Crystallogr., Sect. D* **1993**, *D49*, 18−23. (c) Sheldrick, G. M.; Schneider, T. R. *Methods Enzymol.* **1997**, *277*, 319−343.

(41) R1 = $\sum(|F_o| - |F_c|)/\sum|F_o|$; wR2 = $[(\sum w(F_o^2 - F_c^2)^2/\sum w(F_o^2)^2]^{1/2}$.

(42) van Eldik, R.; Gaede, W.; Wieland, S.; Kraft, J.; Spitzer, M.; Palmer, D. A. *Rev. Sci. Instrum.* **1993** *64* (5), 1355.

(43) Jaguar 4.0 solves the Schrödinger equation iteratively using SCF methods to calculate the lowest-energy wave function within the space spanned by the basis set. The fundamental integrals are, however, computed in physical space on a grid rather than in the spectral space defined by the basis functions, affording a sizable speed increase for large systems.

(44) Friesner, R. A. *Chem. Phys. Lett.* **1985**, *116*, 39.

(45) Friesner, R. A. *Annu. Rev. Phys. Chem.* **1991**, *42*, 341.

(46) Becke, A. D. *J. Chem. Phys.* **1993**, *98*, 5648.

(47) Hay, P. J.; Wadt, W. R. *J. Chem. Phys.* **1985**, *82*, 299.

(48) *Jaguar 4.0*; Schrödinger, Inc.: Portland, Oregon, 2000.

(49) Rassolov, V. A.; Pople, J. A.; Ratner, M. A.; Windus, T. L. *J. Chem. Phys.* **1998**, *109*, 1223.

(50) Francl, M. M.; Pietro, W. J.; Hehre, W. J.; Binkley, J. S.; Gordon, M. S.; DeFrees, D. J.; Pople, J. A. *J. Chem. Phys.* **1982**, *77*, 3654.

(51) Aldridge, T. K.; Stacy, E. M.; McMillin, D. R. *Inorg. Chem.* **1994**, *33*, 722.

(52) ORTEP-3 for Windows: Farrugia, L. J. *J. Appl. Crystallogr.* **1997**, *30*, 565. This program is based on ORTEP-III v1.02: Burnett, M. N.; Johnson, C. K.*ORTEP-III*, v1.02; Report ORNL-6895; Oak Ridge National Laboratory: Oak Ridge, TN, 1996.

(53) Glendening, M. E. D.; Badenhoop, J. K.; Reed, A. E.; Carpenter, J. E.; Weinhold, F. *NBO 4.0*; Theoretical Chemistry Institute, University of Wisconsin: Madison, WI, 1999.

(54) *HyperChem 5.02*; Hypercube, Inc.: Gainesville, FL, 1996.

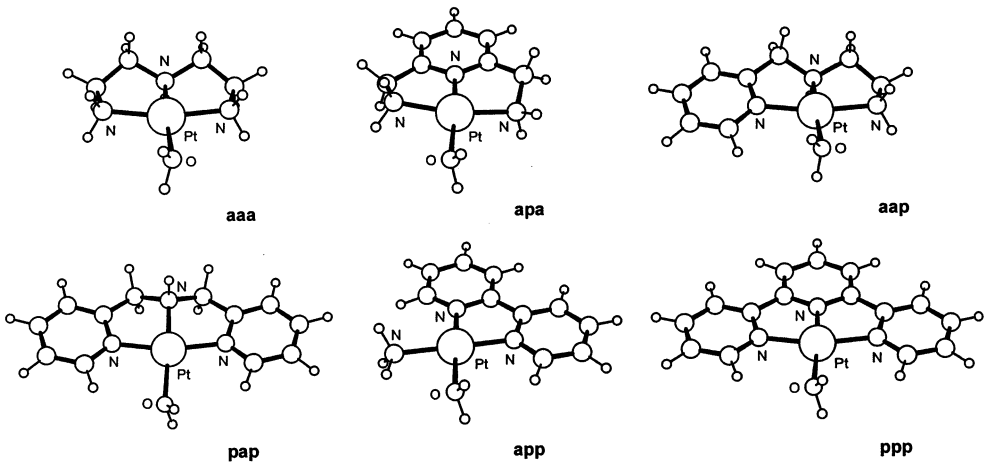

Figure 1. DFT-calculated minimum energy structures for Pt(II) aqua complexes of the type $[Pt^{II}(L)(OH_2)]^{2+}$, where L represents a tridentate N-donor chelate or bipy/NH_3.

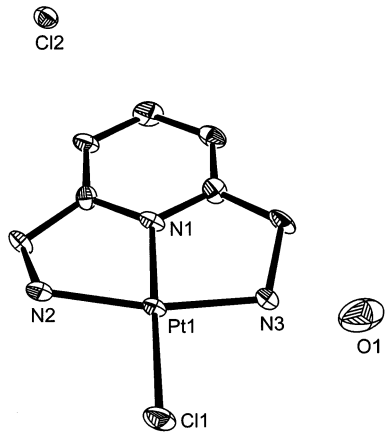

Figure 2. ORTEP plot of the complex [Pt(2,6-bis-aminomethylpyridine)-Cl]Cl·H_2O. Thermal ellipsoids are shown at the 30% probability level. Hydrogen atoms have been omitted for clarity.

4.0 for production level calculations. Minimum energy structures for the nucleophiles TU, DMTU, TMTU, and SCN^- were calculated using PM3[55,56] and their van der Waals volumes (as well as that of I^-) computed within HyperChem using standard methods.

Results

In order to investigate the effect of adding π-acceptor units to tris(N-donor) chelates on the water substitution rates in divalent platinum complexes, a total of six mono(aqua) Pt(II) derivatives were synthesized and characterized. Their DFT-calculated structures are shown in Figure 1. In the case of 2,6-bis-aminomethylpyridine as chelate, the crystal structure of the chloro complex [Pt(2,6-bis-aminomethylpyridine)-Cl]Cl·H_2O was determined and is shown in Figure 2. Table 1 lists selected bond lengths and angles for the structure at room temperature. The mean Pt−N bond distance to the amine nitrogens measures 2.051(6) Å, and the Pt−N distance to the pyridine nitrogen is significantly shorter at 1.932(8) Å. The mean *cis* N−Pt−N angle measures 82.7(2)°; the *trans* N−Pt−N angle is significantly smaller than 180° at 165.4-(3)°. The *trans* N−Pt−Cl angle is, within four standard deviations, linear (179.2(3)°), and the Pt−Cl bond measures

Table 1. Selected Crystallographic Bond Distances and Angles for [Pt(2,6-Bis-aminomethylpyridine)Cl]Cl·H_2O at 293(2) K[a]

	Bond Distances (Å)		
Pt1−N1	1.932(8)	Pt1−N3	2.055(9)
Pt1−N2	2.046(8)	Pt1−Cl1	2.312(3)
	Bond Angles (deg)		
N1−Pt1−N2	82.5(3)	N1−Pt1−Cl1	179.2(3)
N1−Pt1−N3	82.9(3)	N2−Pt1−Cl1	96.8(2)
N2−Pt1−N3	165.4(3)	N3−Pt1−Cl1	97.9(2)

[a] The esd's of the least significant digits are given in parentheses.

2.312(3) Å. The two *cis* N−Pt−Cl angles average 97.4(8)°, consistent with the departure from a perfect square-planar coordination sphere (all angles = 90°) as a result of the geometric constraints imposed by coordination to the tridentate chelate. The sum of the angles subtended at the Pt(II) ion is 360.1°, indicating a planar coordination sphere, which is also proven by the torsion angles. The structural parameters of the coordination sphere (bonds and angles) are in agreement with those observed for similar Pt(II) derivatives, including $[Pt(dien)Cl]^+$ (e.g., *trans* N−Pt−N = 165.4(4)°, Pt−Cl = 2.312(3) Å)[57] and $[Pt(terpy)Cl]^+$ (e.g., *trans* N−Pt−N = 161.8(2)°, Pt−Cl = 2.307(1) Å).[58]

The similarities and differences between the aqua complexes **aaa**, **aap**, **apa**, **pap**, **app**, and **ppp** were first studied by determining the pK_a values of the coordinated water molecules, followed by a study of the ligand substitution reactions as a function of nucleophile concentration for different nucleophiles, pH, temperature, and pressure. These measurements resulted in rate constants and activation parameters ($\Delta H^‡$, $\Delta S^‡$ and $\Delta V^‡$) for the replacement of coordinated water. DFT calculations involving structure determination, calculation of the electron density around the Pt(II) center, and calculation of the frontier molecular orbital energies were also performed. A preliminary report on this study was published elsewhere.[27]

Thermodynamic Studies. Preparation of Complex Solutions. Aqueous solutions of the complexes were pre-

(55) Stewart, J. J. P. *J. Comput. Chem.* **1989**, *10*, 209.
(56) Stewart, J. J. P. *J. Comput. Chem.* **1989**, *10*, 221.
(57) Britten, J. F.; Lock, C. J. L.; Pratt, W. M. C. *Acta Crystallogr., Sect. B* **1982**, *B38*, 2148.
(58) Yip, H.-K.; Cheng, L.-K.; Cheung, K.-K.; Che, C.-M. *J. Chem. Soc., Dalton Trans.* **1993**, 2933.

Table 2. Summary of the Second-Order Rate Constants for the Replacement of Water by a Range of Nucleophiles in Complexes of the Type $[Pt^{II}(L)(OH_2)]^{2+}$

	k_1, $M^{-1}\,s^{-1}$					
nucleophile	**aaa**	**apa**	**aap**	**pap**	**app**	**ppp**/10^4
TU[b]	29.1 ± 0.4	101 ± 1	110 ± 1	393 ± 2	1429 ± 6	16.3 ± 0.2
DMTU[c]	11.9 ± 0.2	41.2 ± 0.3	80.4 ± 0.5	393 ± 5	1690 ± 21	21.7 ± 0.3
TMTU[d]	3.20 ± 0.02	12.3 ± 0.1	29.3 ± 0.2	182 ± 2	1196 ± 29	15.3 ± 0.3
I^-	67.3 ± 0.5	180 ± 1	246 ± 2	854 ± 6	1690 ± 21	22.4 ± 0.4
SCN^-	40.4 ± 0.5	88.3 ± 0.5	115 ± 1	367 ± 6	953 ± 17	11.9 ± 0.1
Cl^-		1.91 ± 0.01	2.29 ± 0.01			
Br^-		10.4 ± 0.1	13.9 ± 0.1			

	pK_a					
	aaa	**apa**	**aap**	**pap**	**app**	**ppp**
pK_a[e]	6.35 ± 0.03	5.96 ± 0.05	5.60 ± 0.06	5.30 ± 0.03	4.37 ± 0.02	4.42 ± 0.05
pK_a[f]	6.26 ± 0.10	6.04 ± 0.08	5.71 ± 0.03	5.53 ± 0.07	4.68 ± 0.03	4.62 ± 0.04

[a] Kinetic and thermodynamic pK_a values for platinum-bound water in these complexes are also given. Experimental conditions: ionic strength = 0.1 M ($NaClO_4$), 25 °C, pH = 2.0−2.5. [b] Thiourea. [c] Dimethylthiourea. [d] Tetramethylthiourea. [e] Kinetic value. [f] Thermodynamic value.

pared by dissolving known amounts in 0.1 M $HClO_4$. Thus, the pH was 1.0, the ionic strength was 0.1 M, and the starting complex was in its aqua form. The concentration selected for each complex was based on its UV−vis spectrum, making sure that the peak(s) of interest had a minimum absorbance of 0.6 units. The solubility of the complexes was very different; for instance, the **ppp** complex took much longer to dissolve than the **aaa** complex.

Thermodynamic Studies. Acidity and Formation of Hydroxo Complexes. Spectrophotometric pH titrations of the complex solutions were performed with NaOH as the base at 25 °C. To avoid absorbance corrections due to dilution, a large volume (300 mL) of the complex solution was used in the titration. A change in pH from 1 to approximately 2 was achieved by addition of known amounts of crushed pellets of NaOH. The consecutive pH changes were obtained by adding drops of saturated solutions of NaOH, 1 or 0.1 M NaOH using a micropipet. It was found that when the pH electrode (filled with NaCl instead of KCl to avoid precipitation of $KClO_4$) was dipped into the solution for a long time, it resulted in the formation of a red precipitate that was suspected to be the chloro complex. It was therefore necessary to take 2 mL aliquots from the solution into narrow vials for the pH measurements, which were discarded after the measurement. The total reversibility of the titration could be achieved by subsequent addition of $HClO_4$.

A typical example of the spectral changes observed during the pH titration is shown in Figure 3. The spectra are characterized by two or more isosbestic points, which are maintained to the end of the titration. This suggests that there are only two species present in solution as a function of pH, viz. the aqua and hydroxo complexes. The overall process can therefore be presented by reaction 1.

$$\text{“L3”}Pt^{II}\text{-}OH_2^{2+} + H_2O \overset{K_a}{\rightleftharpoons} \text{“L3”}Pt^{II}\text{-}OH^{+} + H_3O^{+} \quad (1)$$

Plots of absorbance versus pH at specific wavelengths were used to determine the pK_a value of the coordinated water molecule. The data points were fitted using a nonlinear least-squares procedure, and the plots are shown as insets in Figure 3. The pK_a values are summarized in Table 2.

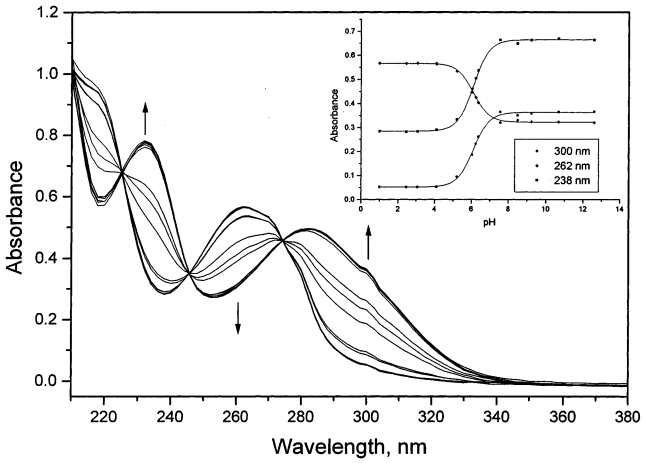

Figure 3. Electronic spectra for the **apa** complex in the pH range 1−10; I = 0.1 M ($NaClO_4$), T = 25 °C. Inset: Plot of absorbance versus pH at the specified wavelengths.

Kinetic Measurements. The kinetics of the substitution of coordinated water (reaction 2) were followed spectrophotometrically by following the change in absorbance at suitable wavelengths (Table S1) as a function of time using the stopped-flow technique. A total of five, neutral and anionic, nucleophiles, viz. thiourea (TU), *N*,*N*-dimethylthiourea (DMTU), *N*,*N*,*N*′,*N*′-tetramethylthiourea (TMTU), iodide, and thiocyanate, which have different nucleophilicities and steric hindrance, were used as incoming ligands.

$$\text{“L3”}Pt^{II}\text{-}OH_2^{2+} + Nu^{n-} \underset{k_{-1}}{\overset{k_1}{\rightleftharpoons}} \text{“L3”}Pt^{II}\text{-}Nu^{(2-n)+} + H_2O \quad (2)$$

All kinetic experiments were performed under pseudo-first-order conditions, and at a pH between 2.0 and 2.5, where the complexes exist in the aqua form based on the data in Table 2. The ionic strength of the reaction mixtures was kept constant at 0.1 M with $NaClO_4$.

The kinetic traces gave excellent fits to a single exponential. The so-obtained pseudo-first-order rate constants, k_{obsd}, were plotted against the concentration of the entering nucleophile. A linear dependence on the nucleophile concentration with no meaningful intercept was observed for all reactions. Plots showing representative results for one

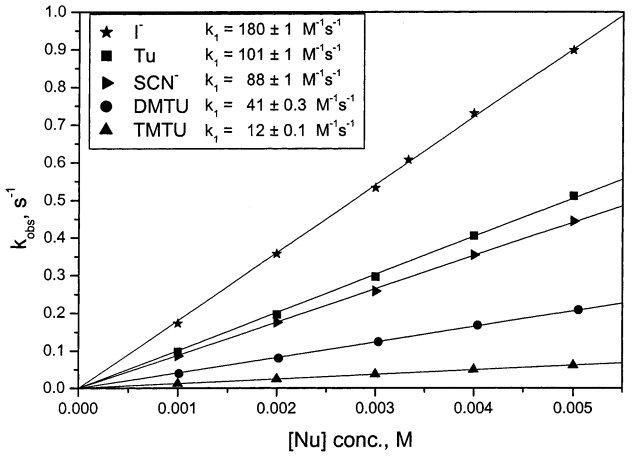

Figure 4. Plots of k_{obsd} versus nucleophile concentration for the **apa** complex. $I = 0.1$ M ($NaClO_4$), $T = 25$ °C, pH = 2 ($HClO_4$).

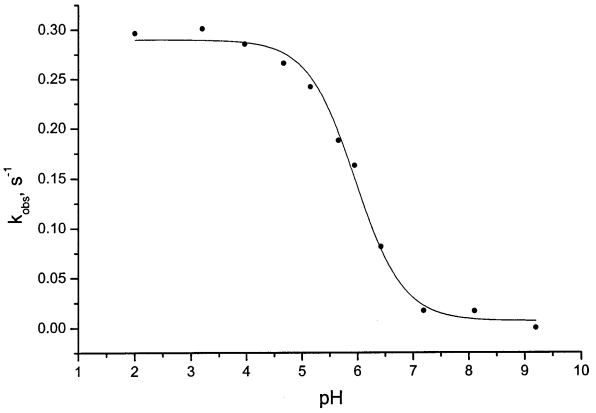

Figure 5. pH dependence of k_{obsd} for the reaction between the apa complex and thiourea at 25 °C, $I = 0.1$ M ($NaClO_4$), [**apa**] = 0.1 mM, $\lambda = 300$ nm.

complex are shown in Figure 4. The results imply that k_{obs} can be expressed by eq 3.

$$k_{obsd} = k_1[\mathrm{Nu}] + k_{-1} \approx k_1[\mathrm{Nu}] \qquad (3)$$

In the case of strong nucleophiles, the reaction is irreversible and $k_{-1} \approx 0$. For the reaction involving the weak nucleophile sulfate, a significant contribution of a back reaction was observed, viz. **aaa**, $k_1 = 4.6 \pm 0.8$ M^{-1} s^{-1}, $k_{-1} = (0.6 \pm 0.1) \times 10^{-2}$ s^{-1}; **pap**, $k_1 = 32 \pm 5$ M^{-1} s^{-1}, $(k_{-1} = 0.5 \pm 0.1) \times 10^{-2}$ s^{-1}; **ppp**, $k_1 = 2470 \pm 630$ M^{-1} s^{-1}, $k_{-1} = (21 \pm 1) \times 10^{-2}$ s^{-1}. These reactions were studied at a pH of 2.5, where the nucleophile is at least 80% SO_4^{2-} and ca. 20% HSO_4^- for a pK_a value of 1.89 for HSO_4^-.[59]

The substitution reactions of the complexes with thiourea (TU) were studied over the entire pH range in order to determine the pK_a values kinetically. The coordinated water molecule on Pd(II) and Pt(II) centers has been shown to be very labile and can easily be substituted compared to stronger nucleophilic leaving groups.[60] However, following deprotonation, the resulting hydroxo ligand was found to be practically inert to substitution, presumably due to a back-

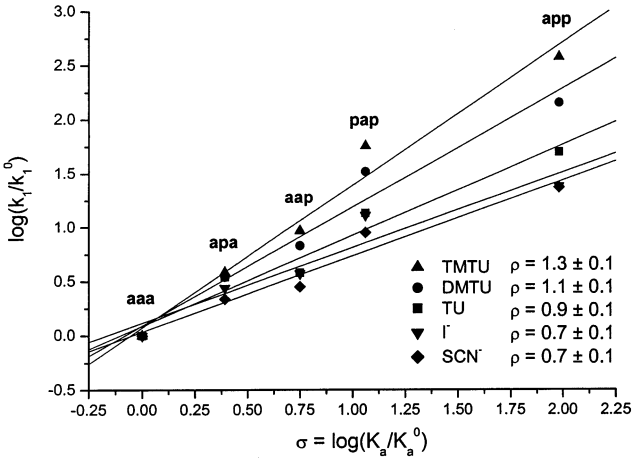

Figure 6. Hammett plot of $\log(k_1/k_1^0)$ versus $\log(K_a/K_a^0)$ according to eq 5 for the aqua complexes at 25 °C for the entering nucleophiles I^-, SCN^-, TU, DMTU, and TMTU. The values for **aaa** were used as reference (k_1^0, K_a^0).

Scheme 1

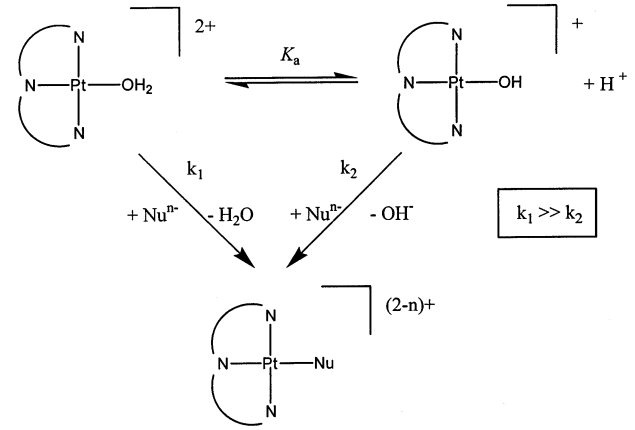

bonding effect of the lone pair electrons on the hydroxo ligand with the p_z orbital of the metal, by which the Pt−OH bond obtains a quasi-double-bond character.[61,62] This phenomenon was also observed in the systems studied here. The substitution process can therefore be represented by the mechanism outlined in Scheme 1.

The rate law for this mechanism is given by eq 4. The resulting pH profile for the **apa c**omplex fitted using eq 4 is shown in Figure 5, and the calculated pK_a values are summarized in Table 2.

$$k_{obsd} = \left\{\frac{k_1[\mathrm{H}^+] + k_2K_a}{K_a + [\mathrm{H}^+]}\right\}[\mathrm{Nu}] \qquad (4)$$

The agreement with the thermodynamically determined pK_a values is, within the experimental error limits, rather good. These values can be related to the second-order rate constant, k_1, by a Hammett plot as shown in Figure 6.

The activation parameters were determined through a systematic variation of temperature and pressure. The thermal activation parameters $\Delta H^{\ddagger}$ and $\Delta S^{\ddagger}$ were calculated using the Eyring equation, and the data are summarized in Table

(59) Holleman, A. F.; Wiberg, E.; Wiberg, N. *Lehrbuch der anorganischen Chemie*; de Gruyter: Berlin, 1995; p 585.
(60) Kotowski, M.; van Eldik, R. In *Inorganic High-Pressure Chemistry. Kinetics and Mechanisms*; van Eldik, R., Ed.; Elsevier: Amsterdam, 1986; Chapter 4.
(61) Mahal, G.; van Eldik, R. *Inorg. Chem.* **1985**, *24*, 4165.
(62) Mahal, G.; van Eldik, R. *Inorg. Chim. Acta* **1987**, *127*, 203.

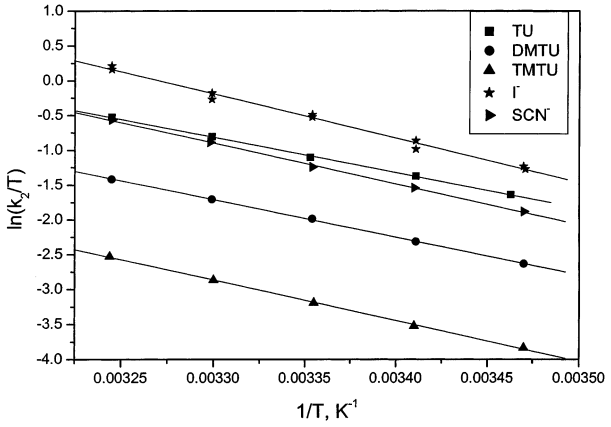

Figure 7. Eyring plots for the determination of the activation enthalpies and entropies for the reactions of the **apa** complex with different nucleophiles.

Table 3. Activation Parameters for the Reaction of Different Nucleophiles with $[Pt^{II}(L)(OH_2)]^{2+}$ at 25 °C

chelate L	nucleophile	$\Delta H^{\ddagger}$, kJ mol^{-1}	$\Delta S^{\ddagger}$, JK^{-1} mol^{-1}	$\Delta V^{\ddagger}$, cm^3 mol^{-1}
aaa	TU	44.2 ± 1.1	−69 ± 4	−6.0 ± 0.1
	DMTU	52.0 ± 1.5	−50 ± 5	−8.9 ± 0.4
	TMTU	62.9 ± 1.4	−11 ± 5	−8.8 ± 0.7
	I^-	53.7 ± 0.7	−30 ± 2	
	SCN^-	55.6 ± 1.1	−29 ± 4	
apa	TU	42.3 ± 0.7	−65 ± 2	−5.3 ± 0.6
	DMTU	45.0 ± 0.5	−63 ± 2	−6.9 ± 0.4
	TMTU	48.4 ± 0.8	−62 ± 3	−10.3 ± 1.4
	I^-	51.6 ± 0.3	−29 ± 1	
	SCN^-	48.7 ± 0.9	−45 ± 3	
aap	TU	42.2 ± 1.0	−65 ± 3	−5.3 ± 0.5
	DMTU	44.7 ± 0.9	−59 ± 3	−8.5 ± 0.9
	TMTU	44.4 ± 0.9	−68 ± 3	−9.1 ± 0.8
	I^-	49.7 ± 1.1	−33 ± 4	
	SCN^-	49.3 ± 0.2	−40 ± 1	
pap	TU	40.1 ± 0.4	−61 ± 1	−6.8 ± 0.3
	DMTU	46.2 ± 1.7	−41 ± 6	−6.3 ± 0.4
	TMTU	43.2 ± 1.7	−57 ± 6	−8.2 ± 0.4
	I^-	46.2 ± 0.7	−41 ± 1	
	SCN^-	46.9 ± 1.2	−46 ± 5	
app	TU	36.4 ± 0.5	−63 ± 2	−6.0 ± 1.3
	DMTU	38.2 ± 0.5	−56 ± 2	−6.1 ± 1.1
	TMTU	41.1 ± 0.6	−48 ± 2	−8.0 ± 0.8
	I^-	49.8 ± 0.6	−14 ± 2	
	SCN^-	48.9 ± 1.4	−24 ± 4	
ppp	TU	21.5 ± 0.3	−73 ± 1	−6.0 ± 0.4
	DMTU	17.6 ± 0.4	−84 ± 1	−6.5 ± 0.4
	TMTU	18.9 ± 0.4	−82 ± 1	−8.1 ± 0.1
	I^-	30.3 ± 1.1	−47 ± 4	
	SCN^-	31.3 ± 0.9	−52 ± 3	

3. Figure 7 shows typical Eyring plots for **apa**. The effect of high pressure was studied only for the neutral entering nucleophiles to avoid possible volume changes associated with changes in electrostriction. The **ppp** complex is extremely reactive, and the reaction rates are close to the dead time of the high-pressure stopped flow instrument. Experiments for this complex were, therefore, repeated 16 times for each nucleophile at each pressure, instead of 8 times as for all the other complexes. The values of k_{obsd} increased with increasing pressure, and the dependence of ln(k_{obsd}) on the applied pressure was linear as can be seen from the selected plots in Figure 8. The calculated volumes of activation, $\Delta V^{\ddagger}$, are summarized in Table 3. The acceleration of the reaction by pressure is indicative of an associative substitution mechanism. This is also supported by the

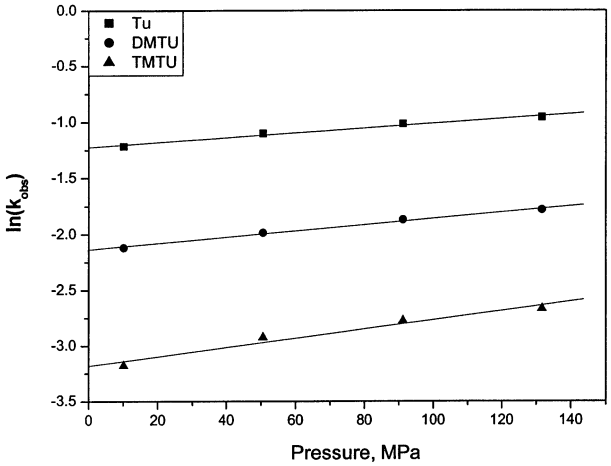

Figure 8. Plots of ln(k_{obs}) vs pressure for the reaction of the **apa** complex with the neutral nucleophiles TU, DMTU, and TMTU: $I = 0.1$ M ($NaClO_4$), pH = 2 ($HClO_4$), $T = 25$ °C, [**apa**] = 0.1 mM.

Table 4. DFT-Calculated (B3LYP/LACVP**) Structural and Electronic Parameters for Pt(II) Complexes of the Type $[Pt^{II}(L)(OH_2)]^{2+}$

complex	Pt charge (e)	Pt−O bond length (Å)	N−Pt−N angle sum (deg)[a]	E_{HOMO} (eV)	E_{LUMO} (eV)	ΔE (eV)
aaa	0.7415	2.149	168.32	−15.1865	−9.7695	5.4170
apa	0.7732	2.153	164.14	−14.7721	−9.3992	5.3729
aap	0.7669	2.149	166.75	−14.5305	−9.2797	5.2508
pap	0.7910	2.151	165.69	−14.0616	−8.8634	5.1982
app	0.7931	2.157	179.27	−13.9976	−9.4264	4.5713
ppp	0.8273	2.163	162.22	−13.5201	−9.3866	4.1334

[a] This value is the sum of the two *cis* N−Pt−N angles in each complex.

negative $\Delta S^{\ddagger}$ values calculated from the temperature dependence of the reactions.

DFT Calculations. Minimum-energy structures (full geometry optimizations) calculated at the B3LYP/LACVP** level of theory for the complexes **aaa**, **aap**, **apa**, **app**, and **ppp** are shown in Figure 1, as already noted. The calculated geometries are acceptable given the degree of similitude between the X-ray and DFT-calculated structures of [Pt(terpy)(OMe)]$^{+}$ [51] and [Pt(2,6-bis-aminomethylpyridine)Cl]$^{+}$. More specifically, the RMS differences (non-H atoms) between the calculated and X-ray structures were 0.111 and 0.073 Å for these two cations, respectively. Furthermore, the calculated and observed coordination bond distances and angles were in agreement to within 0.08 Å. For [Pt(terpy)(OMe)]$^{+}$, the relevant bonds and distances were (calcd, obsd): Pt−N_1 (1.96, 1.91 Å), Pt−N_2 (2.02, 2.04 Å), Pt−N_3 (2.02, 2.10 Å), and Pt−O (2.08, 2.00 Å). In the case of [Pt(2,6-bis-aminomethylpyridine)Cl]$^{+}$, crystal packing effects were negligible, and a somewhat better agreement between the calculated and observed coordination distances was obtained (calcd, obsd): Pt−N_1 (1.99, 1.95 Å), Pt−N_2 (2.09, 2.02 Å), Pt−N_3 (2.09, 2.01 Å), Pt−Cl (2.334, 2.323 Å). Table 4 summarizes the calculated N−Pt−N bond angles, Pt−O bond lengths, and the electron density around the Pt(II) center for each derivative. The energies of the frontier molecular orbitals of the complexes are also given. It can clearly be seen that, in going from **aaa** to **pap**, the LUMO energy rises in a manner quite similar to the HOMO energy, but the increase in the latter is slightly higher. A significant decrease in the LUMO energy is observed from **pap** to **app** because

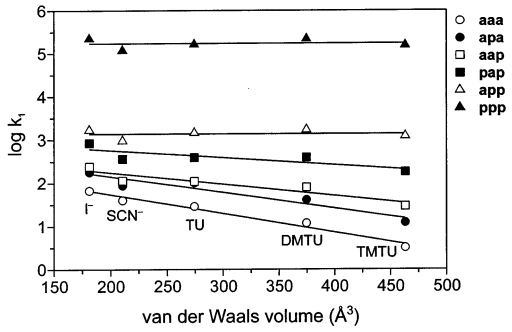

Figure 9. Plot of log k_1 for the replacement of water in six $[Pt(L)(OH_2)]^{2+}$ derivatives against the calculated van der Waals volumes of the incoming nucleophiles I^-, SCN^-, TU, DMTU, and TMTU.

of the linkage of two aromatic rings in the latter complex, whereas the introduction of a third pyridine ring (from **app** to **ppp**) results in a significant increase in the HOMO energy. The energy gap between HOMO and LUMO decreases along the series. The changes in energy are relatively small for the **aaa**, **apa**, **aap**, and **pap** complexes (about 0.1 eV), but a large decrease in ΔE is observed for **app** and **ppp** (0.5 eV in each case), which can be accounted for in terms of the extended aromatic system induced by the adjacent aromatic rings. Another trend that can be observed is an increase in the positive NBO charge on Pt(II) with an increasing number of π-acceptors on the complex.

Figure 9 shows plots of log k_1 for the displacement of water in the complexes **aaa**, **aap**, **apa**, **pap**, **app**, and **ppp** versus the calculated van der Waals volumes (a measure of steric bulk) of the incoming nucleophiles I^-, SCN^-, TU, DMTU, and TMTU. The plots for **app** and **ppp** have zero slopes, indicative of a substitution process that is essentially independent of steric effects. The steepest slope is observed for the dien derivative **aaa**. The log k_1 values for **aaa**, **apa**, **aap**, and **pap** therefore show a clear dependence on the steric bulk of the entering nucleophile, with the fastest and slowest substitution rates being observed for the smallest (I^-) and largest (TMTU) nucleophiles, respectively.

Discussion

In this study, two new Pt(II) complexes of **apa** and **aap** have been synthesized and spectroscopically characterized. We have, in addition, obtained a novel single crystal X-ray structure of the chloro precursor of the Pt(II) **apa** aqua complex, namely [Pt(2,6-bis-aminomethylpyridine)Cl]Cl·H_2O. A new synthetic route for the tridentate ligand 2,6-bis-aminomethylpyridine was also developed. Moreover, aqua Pt(II) complexes of **apa**, **aap**, **pap**, and **app** were synthesized for the first time. As far as we know, this is the first systematic and comparative study of the selected complexes performed under similar experimental conditions.

Ionization of Platinum Bound Water. The thermodynamic data in Table 2 demonstrate that there is a remarkable correlation between the pK_a values for the coordinated water molecule and the structure, especially the π-acceptor character of the individual spectator ligands; the more π-acceptors in the system, the lower the pK_a value. This can be explained in terms of the electron withdrawing ability of each added pyridine ring, which controls the electrophilicity of the metal center and stabilizes the negatively charged hydroxo ligand.

Although it is not a novel finding that the pK_a value of coordinated water is an experimental indicator of the electron density around the metal center,[63] it is interesting that, in all of the complexes except **ppp**, the pK_a value is an experimental gauge of the lability of the aqua complex (as shown by the Hammett plot in Figure 6, vide infra). This experimental finding is paralleled by a similar, though not perfect, trend in the DFT-calculated charges on the Pt(II) ion. The DFT calculations show that each addition of a pyridine ring to the system increases the NBO charge on the Pt(II) ion by about 0.03 units (Table 4). This reveals how each π-acceptor modulates the electron density at the metal center and modulates its electrophilic character. However, it is astonishing that the effect on the charge of the Pt center is that small, considering the rather large effects on the substitution rates and pK_a values. We suggest that the NBO charges in the ground state become more positive because of the interaction between the d_{xz} and d_{yz} orbitals with the empty anti- or nonbonding ligand orbitals. This effect is rather small compared to the ability of the π-acceptors to stabilize additional incoming electron density in the p_z orbital of the Pt metal center, i.e., to stabilize the hydroxo ligand or the additional electrons from the entering nucleophile in the transition state during associative ligand substitution.

It can be seen from the kinetic studies performed as a function of pH that the reactivity of the investigated complexes is highly pH dependent since the hydroxo species is mostly substitution inert compared to the highly reactive aqua species (see for example Figure 5). This kinetic behavior can be expressed by eq 4. Thus, if the pH of the solution is significantly lower than the pK_a value of the complex, the substitution kinetics will be fast, whereas if the pH is significantly higher, the complex is inert. In general the kinetically determined pK_a values are in good agreement with the thermodynamically determined ones. Only for the more labile complexes **pap**, **app**, and **ppp** is the kinetically determined pK_a value slightly (0.2−0.3 pK_a units) lower than the thermodynamic value.

Reactivity and π-Acceptor Ability. From a comparison of the reactivity of the aqua complexes in Table 2, it can be seen that the substitution behavior of the complexes clearly depends on the π-acceptor properties of the selected ligands. The introduction of pyridine groups into the **aaa** complex significantly increases the π-acceptor abilities of the chelate. The net outcome is a significant increase in the electrophilicity of the metal center, as reflected by a more positive charge on the Pt(II) ion and a lower pK_a for the ionization of the aqua ligand. This results in an increase in the substitution rate of coordinated water.

For the reaction with thiourea (TU), the rate of substitution increases by a factor of 4 in going from **aaa** to **aap**, with a further enhancement by a factor of approximately 4 on the addition of a second pyridine ring (**pap**). On going from **aaa**

(63) Dadci, L.; Elias, H.; Frey, U.; Hörnig, A.; Koelle, U.; Merbach, A. E.; Paulus, H.; Schneider, J. S. *Inorg. Chem.* **1995**, *34*, 306.

to **app** and **ppp**, the substitution rate increases by 2 and 4 orders of magnitude, respectively. The reason for this enhanced reactivity is π-back-donation of the additional electron density from the entering nucleophile to the chelate ligand, which stabilizes the five-coordinate transition state in comparison to the ground state,[9] which cannot benefit that much from the π-back-donation since the $6p_z$ orbital of the Pt center is empty. This increases its electrophilicity and reactivity toward entering nucleophiles.

Interestingly, our observed reactivity order for the Pt(II) aqua complexes, viz. **aaa** < **apa** < **aap** < **pap** < **app** < **ppp**, is in good agreement with that expected for this series of complexes, but only partly matches that reported for substitution reactions of the analogous chloro complexes in methanol by Pitteri et al.[28] These workers found that [Pt(bis(2-pyridylmethyl)amine)Cl]$^+$ reacts slower than [Pt(2,6-bis-aminomethylpyridine)Cl]$^+$, which contradicts our findings for the reactions of the corresponding aqua complexes. This may be related to the fact that they investigated the reactions of the chloro complexes in methanol as solvent, such that the two studies are not that compatible.

From the observed reactivity order, the questions remain for how the number and position of the π-acceptor ligands can affect the observed reactivity, and in which way two or three π-acceptor pyridine rings can interact with each other. It seems logical that if the introduction of one π-acceptor in the *cis* position (**aap** as compared to **aaa**) results in an enhancement of about a factor of 3.8 (for TU), the introduction of a second π-acceptor group (**pap**) results in a further acceleration factor of 3.8, i.e., an overall factor of 14.4. From the values in Table 2, it follows that the reaction of **pap** with TU is 13.6 times faster than the reaction of the **aaa** complex with TU. The other nucleophiles behave in a similar way, only the factors that are squared as already shown vary due to the reduced importance of steric hindrance on increasing the electrophilicity of the metal center (see later). It can, therefore, be concluded that the effects of the π-acceptor groups can to some extent be combined in a multiplicative manner.

It is widely accepted in inorganic textbooks that the electronic *trans* effect is much stronger than the electronic *cis* effect in Pt(II) complexes (as soon as steric hindrance plays a role, the importance is reversed).[64] However, this statement is based mainly on investigations with σ-donor ligands or ligands which have both σ-donating and π-accepting properties. It is therefore interesting to compare the influence of only the π-effect (in the absence of a variation of the σ-donor properties) in the *trans* (**apa**) to that in the *cis* position (**aap**). Since the pK_a value for the latter complex is slightly smaller, we would expect a higher reactivity for **aap**. The data in Table 2 show that this expectation is perfectly correct. The k_1 values for the substitution reactions with TU, I^-, and SCN^- are 10−30% higher, and in the case of the sterically hindered nucleophiles DMTU and TMTU, the values are 2 to 3 times higher, respectively. To our knowledge, this is the first time that it is shown that the *cis* effect for a specific ligand can be larger than its *trans* effect, as long as steric hindrance is excluded. The effect can rather easily be accounted for in terms of the orbitals involved. The π-effect results mainly from an interaction between the perpendicular $6p_z$ Pt orbital (accepting additional electron density) and the perpendicular non-/antibonding π-orbitals of the ligands. Since all the involved orbitals are perpendicular to the square-planar plane, the same interaction of the orbitals should occur in the *cis* and *trans* position. This would account for the similar influence of a *cis* or a *trans* aromatic ring on the thermodynamic and kinetic findings but offers no explanation for the enhanced reactivity/decrease in pK_a of the **aap** system (in comparison to **apa**). However, from the DFT-calculated ground state orbitals (Figure 10), it can be seen that in the **apa** complex most electron density of the HOMO is centered above and below the metal center. This leaves the Pt(II) center in the **apa** complex less electrophilic than in the **aap** complex, where the electron density of the HOMO is located more on the ligand. We suggest that these explicit differences in the two HOMO orbitals are due to symmetry reasons. There is a mirror plane of symmetry (σ) (only one if we consider the orbitals, but two if we consider the overall geometry) in the **apa** complex, and no symmetry at all in the **aap** complex. The accumulation of electron density on the Pt(II) center in the case of the **apa** complex leads to a less electrophilic metal center, which results in a higher pK_a and a slower substitution reaction. This then explains why the *cis* effect is slightly larger than the *trans* effect on considering only the π-acceptor interactions. This demonstrates once more[6,65] that it is necessary to distinguish between σ-donor and π-acceptor effects of the ligands when referring to *cis* and *trans* effects.

If we ignore the fact that the *trans* π-acceptor has a slightly smaller influence on the rate than the *cis* π-acceptor, the **pap** and **app** complexes should be comparable in their kinetic and thermodynamic behavior since they both have two π-acceptor rings. However, the opposite was found. The pK_a value for the **app** complex is about 0.9 units lower than that of the **pap** complex, and the rate of substitution is about 2

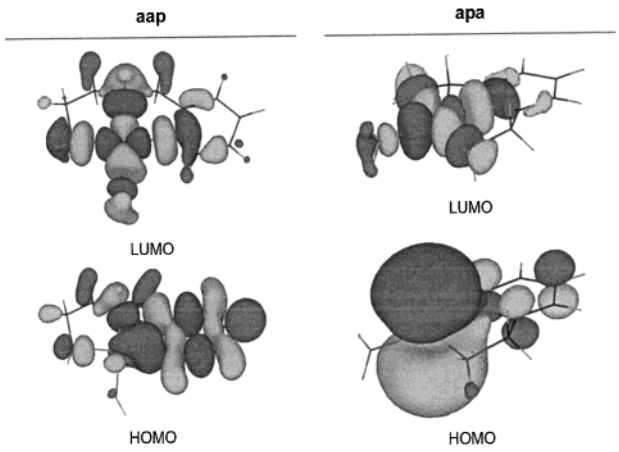

Figure 10. DFT-calculated (B3LYP/LACVP**) HOMOs and LUMOs for the Pt(II) complexes **aap** and **apa**.

(64) Tobe, M. L.; Burgess, J. *Inorganic Reaction Mechanisms*, 1st ed.; Addison-Wesley Longman Limited: Reading, MA, 1999.

(65) Wendt, O. F.; Deeth, R. J., Elding, L. I. *Inorg. Chem.* **2000**, *39*, 5271.

(I^-) to 6 times (TMTU) faster than for **pap**. These data imply that the platinum center is more electrophilic when two pyridine rings are adjacent to each other. We accounted for this effect in terms of "electronic communication" between the ligands that resulted in very efficient π-back-bonding.[27] In the case of the **ppp** complex, the same effect is at hand. Since we now know that the acceleration effect on the addition of π-acceptors is multiplicative (see earlier discussion), it would be reasonable to expect the **ppp** complex to be about 20−226 (**apa** combined with **pap**) times faster than the **aaa** complex, depending on the nature of the entering nucleophile. However, a much larger increase in the rate constant of 3×10^3 to 5×10^4 is observed. This must be due to the effect of efficient electronic communication between the chelate partners. The large increase in the rate constant as compared to the **app** complex can be accounted for by the fact that, in the **ppp** complex, three rings are adjacent to each other instead of only two in the case of the **app** complex. Interestingly, this effect does not show up in the DFT-calculated NBO charges. Here, an effect for each added ring is seen, but no difference between the **pap** and **app** complexes is seen based on the NBO charges. We suggest that the observed changes in the NBO charges are due to the interaction between the $5d_{xz}$ and $5d_{yz}$ metal orbitals with the π-accepting orbitals on the ligand, whereas the observed increase in reactivity is due to the stabilization of the additional electron density in the $6p_z$ orbital in the transition state. Since the calculations, which were done for the ground state of the aqua complexes, show no effect of electronic communication on the NBO charge, we conclude that only the $6p_z$ orbital benefits from this effect. However, looking at the frontier orbital energies, a clear trend can be observed. In the case of electronic communication (**app** and **ppp**), the energy gap ($E_{HOMO} - E_{LUMO}$) is reduced by 0.5 eV for each added "communicating" ring. We propose two possible explanations for the suggested electronic communication between the π-acceptor ligands. First, the orbitals of two neighboring rings interact with each other which results in a smaller HOMO−LUMO gap and a more effective overlap between the π-donating and π-accepting orbitals on the Pt(II) complex, leading to a decrease in electron density on Pt(II). Second, five-membered aromatic ring(s) involving the Pt(II) center can be formed. The creation of aromaticity between the pyridine rings results in a more extensive π-conjugated system, which in turn is able to stabilize entering electron density more effectively by spreading it over the aromatic system. This effect is much larger for the **ppp** than for the **app** complex. Both explanations may contribute to some extent. It is clear that electronic communication contributes to the thermodynamic and kinetic parameters in addition to the pure π-acceptor effects of single pyridine rings.

Using the Swain−Scott relationship[66] for the nucleophiles Cl^-, Br^-, and I^-, the nucleophilic discrimination factor s can be calculated for the **aap** and **apa** systems. In both cases, the value of s is 0.8 ± 0.1 and therefore much higher than for **aaa** ($s = 0.4 \pm 0.1$), which can be accounted for by the better π-accepting abilities of **aap** and **apa** that affect the nucleophilic discrimination.[67] However, there is no difference in s for **apa** and **aap**, showing that the difference in the HOMOs has no effect on the nucleophilic discrimination factor.

Nucleophile Steric Effect. As already mentioned, substitution of coordinated water by the sterically hindered nucleophiles *N*,*N*′-dimethylthiourea (DMTU) and *N*,*N*,*N*′,*N*′-tetramethylthiourea (TMTU) shows a clear dependence on the steric bulk of the nucleophiles. The most sterically hindered nucleophile TMTU reacts significantly slower than the less hindered TU in the case of the **aaa** complex (Table 2). Upon the introduction of one pyridine π-acceptor ring in the *cis* position (**aap**), DMTU becomes nearly as fast as TU, and the rate for TMTU is now only a third of the rate for TU. In the case of the **pap** complex, the rates for both TU and DMTU are within the experimental error limits almost identical, and TMTU is now only about half as fast as TU. Astonishingly, DMTU becomes even faster than TU on going to the **app** or **ppp** complex, and the most sterically hindered TMTU reacts with these complexes as fast as the nonhindered TU. It can be concluded that the effect of steric hindrance on the rate of substitution along the series of complexes from **aaa** to **ppp** decreases and is offset completely by the electronic effects in the case of the **ppp** complex. This conclusion is fully consistent with the plots of the second-order rate constants for the replacement of water against the calculated van der Waals volumes of the incoming nucleophiles (Figure 9). More specifically, both **app** and **ppp** have zero slopes, i.e., zero dependence on the steric bulk of the nucleophile. This trend can be accounted for in terms of the increase in electrophilicity of the Pt(II) center which reaches a maximum for the **ppp** complex, such that the bulkiness of the attacking nucleophiles is compensated for by the higher nucleophilicity of DMTU and TMTU as a result of the inductive effects of the methyl substituents.[68] It should be kept in mind that the displacement of amines by pyridines also reduces the steric hindrance caused by the solvated hydrogen atoms on NH_2R. This is confirmed by the DFT-calculated geometries of the complexes in Figure 1, showing both **app** and **ppp** to be effectively planar, particularly in the region closest to the Pt-bound aqua ligand. However, this effect is not expected to be very significant. Alternatively, the observed changes in reactivity could also be due to different σ-donor abilities of the N-donors on the displacement of amines by pyridines. The σ-donor abilities of amine-N and pyridine-N donors are almost the same, so that the observed kinetic effects must mainly be due to π-acceptor and not to σ-donor effects.

Linear Free-Energy Relationship (LFER). Since both the pK_a value of the coordinated water molecule and the rate of substitution depend on the π-acceptor properties of the

(66) Swain, C. G.; Scott, C. B. *J. Am. Chem. Soc.* **1953**, *75*, 141.

(67) Belluco, U.; Cattalini, L.; Basolo, F.; Pearson, R. G.; Turco, A. *J. Am. Chem. Soc.* **1965**, *87*, 241.

(68) Preliminary calculations using the 6-31g(d) basis set have shown that the charge on the sulphur atom becomes more negative with an increasing number of methyl substituents on the thiourea nitrogen atoms.

ligands, it seems reasonable to expect a correlation between these two quantities. Such a free-energy relationship is known from organic chemistry, where the K_a values of ring-substituted benzoic acids are correlated with their reactivity in substitution reactions.[69] Since this Hammett relationship deals with the same kind of data (K_a and k_1 values), it is reasonable to use this well-known relationship for the interpretation of our inorganic systems. We took the standard Hammett equation[69] (eq 5) and used the data for the **aaa** complex as a reference system for K_a^0 and k_1^0.

$$\log(k_1/k_1^0) = \rho \times \log(K_a/K_a^0) = \rho \times \sigma \qquad (5)$$

The Hammett plot is shown in Figure 6 for all entering nucleophiles and all studied complexes, except for **ppp** which does not fit the linear correlation at all. The linear dependence observed for five of the six complexes has slopes (ρ values) of 0.7 ± 0.1, 0.7 ± 0.1, 0.9 ± 0.1, 1.1 ± 0.1, and 1.3 ± 0.1, for I^-, SCN^-, TU, DMTU, and TMTU as entering nucleophiles, respectively. The positive values of ρ indicate that the reaction is accelerated by the introduction of electron withdrawing groups (π-acceptors) on the chelate. This means that during the reaction an increase in electron density is developed at the reaction center, as would be expected for an associative substitution mechanism. Higher values for ρ indicate that the amount of electron density developed in the transition state is higher. This means that for the present system the inductive effect of the methyl groups on the substituted thioureas increases the electron density that is stabilized in the transition state. Although the Hammett relationship has been used in the past to account for the reactivity trend in substituted Pt(II) terpy complexes by using σ values of the substituents on the terpy ring system,[70] this is, to our knowledge, the first time that the Hammett relationship has been applied to Pt(II) complexes with σ values based on the K_a values of the aqua complexes.

The only exception in the linear correlation is the **ppp** complex, which according to the correlation should have a significantly smaller pK_a value in order to fit in with its much higher reactivity. A possible explanation for this exceptional behavior is that it may be impossible to drain more electron density from the already very electrophilic center in the ground state to further decrease the pK_a value. However, during an associative substitution reaction with an entering nucleophile, the additional electron density can be spread over the total ligand system to stabilize the transition state and result in an enhanced substitution process. The correlation in Figure 6 therefore suggests that it is possible to predict the kinetic behavior of such systems from thermodynamic data and vice versa, as long as one stays within reasonable limits.

Transition State/Activation Parameters. The trend in the reactivity of the complexes of **aaa** to **ppp** can also be seen in the activation enthalpies for the investigated reactions (Table 3). With increasing electrophilicity of the metal center, there is a decrease in the activation enthalpy due to the stabilization of the transition state. This decrease in $\Delta H^‡$ is more pronounced for the **ppp** complex, where a 2-fold decrease in $\Delta H^‡$ is observed for all studied nucleophiles. On the basis of the activation enthalpies, it appears that charged nucleophiles (I^- and SCN^-) do not benefit as much as the neutral nucleophiles from the strong π-acceptor effect of bipy and terpy in case of **app** and **ppp**, respectively. As mentioned in the discussion of the kinetic data, the difference in $\Delta H^‡$ for the nucleophiles TU, DMTU, and TMTU reduces in going from **aaa** to **ppp**.

It is worth emphasizing that the values of the activation entropy, $\Delta S^‡$, and the activation volume, $\Delta V^‡$, are significantly negative for all studied reactions (Table 3). This is consistent with an associative substitution mechanism and a net increase in bond order in the transition state. Minor trends can be observed for these parameters along the series of complexes. The value of the activation entropy for the negatively charged nucleophiles is much smaller than for the neutral nucleophiles. This is ascribed to charge neutralization effects on bond formation in the transition state. The activation volumes were only determined for the neutral entering nucleophiles, since it is well-known that this parameter is also affected by changes in electrostriction as a result of charge neutralization. The reported activation volumes are very typical for associative substitution reactions on square-planar complexes,[60,71−73] where the volume collapse resulting from bond formation with the entering nucleophile is partially offset by a volume increase resulting from a geometric change from square planar to trigonal bipyramidal in forming the five-coordinate transition state. The activation volumes are independent of the nature of the selected chelate but do become more negative for the larger entering nucleophile TMTU. This can be ascribed to a more effective overlap of the van der Waals radii on forming the five-coordinate transition state with the larger nucleophile.

Pt Coordination Group Steric Effects. Our kinetic data (Table 2) indicate that the reactivity of **ppp** is unusually high relative to the other complexes; **app** also shows notably faster substitution kinetics than the other complexes in this series. A similar effect has been reported for $[Pt(terpy)Cl]^+$, where chloride was the leaving group.[26] The enhanced reactivity of this complex was ascribed to coordination group strain engendered by the terpy ring system. From a comparison of the *trans* N−Pt−N angle (165.4(3)°) and the Pt−Cl bond length (2.312(3) Å) of [Pt(2,6-bis-aminomethylpyridine)Cl]$^+$ (Table 1) with the equivalent structural parameters for $[Pt(dien)Cl]^+$ (N−Pt−N = 165.4(4)°, Pt−Cl = 2.312(3) Å)[57] and $[Pt(terpy)Cl]^+$ (N−Pt−N = 161.8(2)°, Pt−Cl = 2.307(1) Å),[58] it can be seen that the differences in the bond angles are only ~4° when the dien complex is compared to the terpy derivative. However, the Pt−Cl distances are the same within the experimental error limits. We do not believe that a total difference of about 4° in the N−Pt−N angles (i.e.,

(69) Hansch, C.; Leo, A.; Taft, R. W. *Chem. Rev.* **1991**, *91*, 165.
(70) Carr, C. A.; Richards, J. M.; Ross, S. A.; Lowe, G. *J. Chem. Res., Synop.* **2000**, *12*, 566.
(71) Stochel, G.; van Eldik, R. *Coord. Chem. Rev.* **1999**, *187*, 329.
(72) Helm, L.; Elding, L. I.; Merbach, A. E. *Helv. Chim. Acta* **1984**, *67*, 1453.
(73) Helm, L.; Elding, L. I.; Merbach, A. E. *Inorg. Chem.* **1985**, *24*, 1719.

ring strain) can account for an acceleration of the rate constants of about 4 orders of magnitude in these complexes. Furthermore, the high reactivity of terpy cannot be ascribed to a ground state labilization of the leaving group due to a strong *trans* σ-donor effect since the Pt−Cl distances remain the same. The DFT-calculated Pt−O bond lengths for the investigated complexes do not agree with this finding; viz. the **ppp** and **app** bond lengths are slightly longer than those for **aaa**, **apa**, **aap**, **pap** (0.003−0.014 Å), suggesting a ground state labilization for **ppp** and **app**. Since the Pt−Cl distance of some corresponding chloro complexes (see previous discussion) do not follow this trend, we believe that the small differences in the calculated bond length are not significant. From the DFT-calculated structural data shown in Table 4 for the analogous aqua complexes, the difference in the N−Pt−N angle sum between **aaa** and **ppp** is only 6°. This value is too small to cause such a large change in reactivity, especially if we consider that from the calculation the **apa** complex (N−Pt−N = 164.1°) is strained ∼4° more than the **aaa** complex (N−Pt−N = 168.3°), and only ∼2° less than the **ppp** complex (N−Pt−N = 162.2°). If steric strain was responsible for the high reactivity of **ppp** (relative to **aaa**), the **apa** system should be more labile than the less strained **aap** and **pap** systems, which is not the case. Finally, if steric strain and not the π-acceptor abilities of the ligands were responsible for the increase in reactivity along the series from **aaa** to **ppp**, the **app** system (which has negligible angular strain within the coordination group since it is only a bidentate ligand) should react slower than the strained **aaa** system, which is clearly not the case. On the basis of these findings, we conclude that strain in the chelate ring plays a negligible role in the acceleration of the investigated substitution reactions.

Conclusions

We have systematically investigated the effect of progressively adding π-acceptor pyridine units to the chelating ligand in $[Pt(L)(OH_2)]^{2+}$ complexes, where L = a tridentate N-donor chelate or NH_3/bipy, without interference from strong σ-donor effects, which normally mask such π-effects. This has led to some unprecedented findings. First of all, the reactivity of the associative substitution reaction on Pt(II) can be increased in a stepwise manner by the addition of π-acceptors. Surprisingly, the experimental findings suggest that the π-*cis* effect is greater than the π-*trans* effect. The classical textbook statement that the "*trans* effect is always larger than the *cis* effect" needs to be reconsidered when π-acceptor ligands are coordinated to Pt(II). Clearly, what may be true for σ-donor ligands does not necessarily apply for ligands with significant π-acceptor ability. This is readily understood in terms of the geometry of the involved orbitals.

The reactivity of these complexes results mainly from the electrophilicity of the metal center, as a result of the electron back-donation of incoming electron density to the ligand orbitals. The electronic communication between the π-acceptor ligands as found in the case of the **app** and **ppp** complexes is responsible for the drastic increase in lability observed in these cases. This is because of their ability to withdraw π-electron density more strongly from the metal center. The effect of breaking this electronic communication between π-acceptor groups has, in fact, been recently shown to lower the substitution rate by a factor of 60.[25] The π-acceptor effects on their own (in the *cis* or *trans* position) are of minor significance in influencing the lability of d^8 square-planar complexes because of the absence of a direct electronic communication. Furthermore, DFT calculations showed that steric strain on the terpy system plays a minor role in controlling reactivity.

Revealed here for the first time is the observation that the rate of substitution is inversely proportional to the basicity of the complex as a whole, and not just that of the leaving or entering groups. This can be correlated with the Hammett relationship, which is usually applied to the reactions in organic compounds. The present investigation also demonstrates that it is possible, through π-acceptor effects, to tune the pK_a and the reactivity of $[Pt(L)(OH_2)]^{2+}$ complexes. Since we have found that the hydroxo species of the tridentate $[Pt(L)OH]^{+}$ derivatives are much less reactive than the corresponding aqua complexes, the pH of the environment can control the reactivity of the complex in terms of the fraction of the aqua complex available in solution. This may prove to be important in terms of the antitumor activity of such complexes, since it is known that cancer cells are distinguishable from normal cells by a difference in the pH of their cytoplasm. We could show by modifying the π-acceptor properties of the spectator ligands that it is possible to tune the pK_a values of the aqua complexes in such a manner that the maximum reactivity is attained under specific pH conditions, for instance in cancer cells. Since one of the reasons for the specific activity of cis-platin against certain cancer cells is the pK_a value of its hydrolysis product in combination with the cell pH, this finding may prove to be important in drug design.

Acknowledgment. The authors gratefully acknowledge financial support from the Deutsche Forschungsgemeinschaft and the Alexander von Humboldt Foundation for a fellowship to D.J. We would also like to express our gratitude to the University of Natal and the NRF (Pretoria) for financial support (D.J. and O.Q.M.).

Supporting Information Available: Table summarizing the selected wavelengths for the kinetic measurements. Crystallographic information in CIF format. This material is available free of charge via the Internet at http://pubs.acs.org.

IC020605R